Supporting Information

3D well-ordered porous phosphorus doped carbon as anode for sodium storage: structure design, experimental and computational Insights

*Yun Qiao,[a,b] Ruimin Han,[a,b] Yudong Pang,[c] Zhansheng Lu,[*c] Jin Zhao,[a,b] Xiaoguang Cheng,[a,b] Huishuang Zhang,[a,b] Zongxian Yang,[c] Shuting Yang[*,a,b] and Yang Liu[*,a]*

[a] School of Chemistry and Chemical Engineering
Henan Normal University, Xinxiang, Henan, 453007 (China)
*E-mail: liuy986@163.com; liuy986@htu.edu.cn; shutingyang@foxmail.com

[b] National and Local Joint Engineering Laboratory of Motive Power and Key Materials
Henan Normal University, Xinxiang, Henan, 453007 (China)

[c] College of Physics and Materials Science, Henan Normal University, Xinxiang 453007, P. R. China
*Email: zslu@henannu.edu.cn

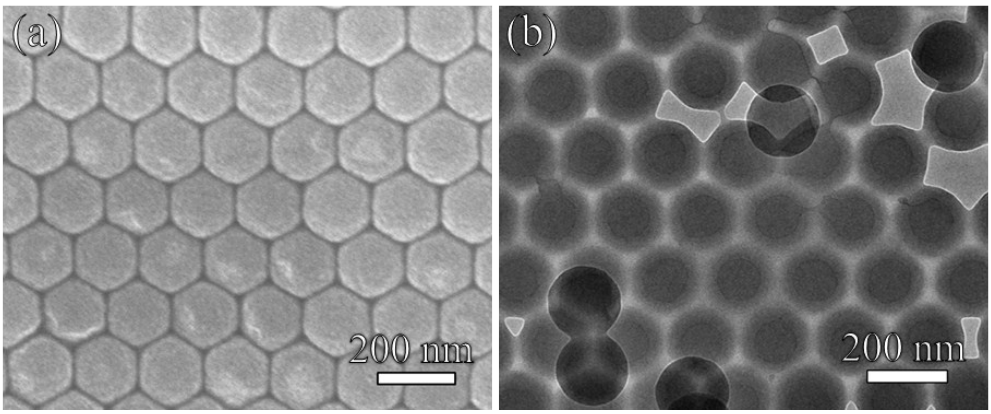

Figure S1. (a) SEM and (b) TEM images of the PS nanospheres, presenting the diameters are of ~170 nm.

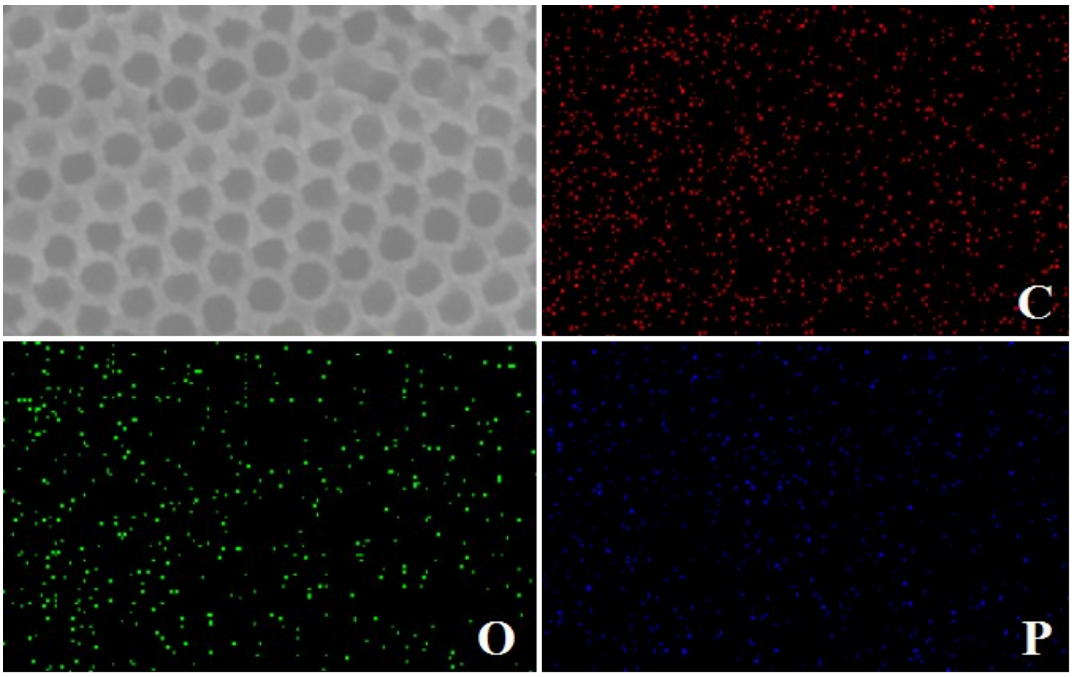

Figure S2. SEM image and the corresponding elemental mapping images of carbon, oxygen and phosphorus for well-ordered 3D porous PC, further indicating the successful doping of phosphorus and uniform distribution of C, O and P.

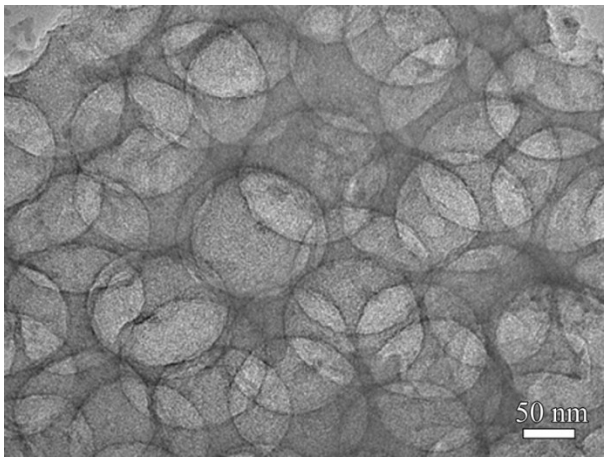

Figure S3. TEM image of the well-ordered 3D porous PC.

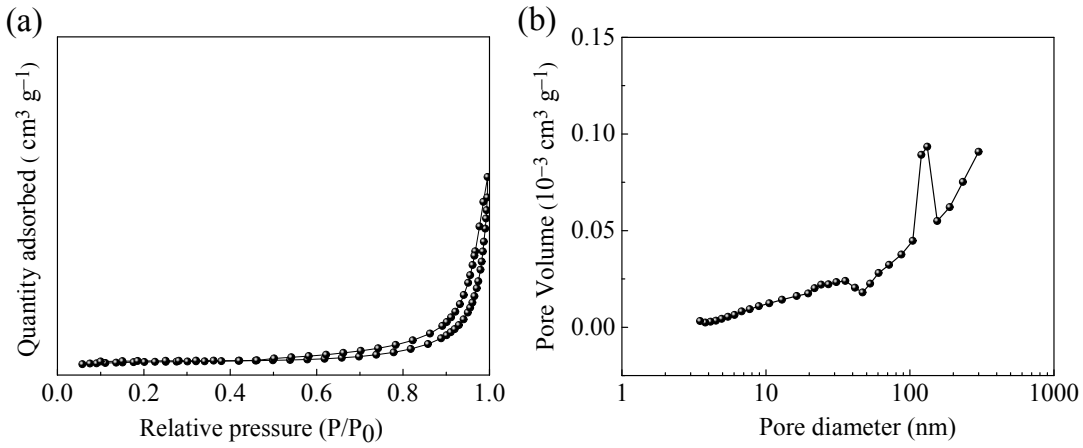

Figure S4. (a) Nitrogen adsorption–desorption isotherms, and (b) pore size distribution (PSD) plots of PC.

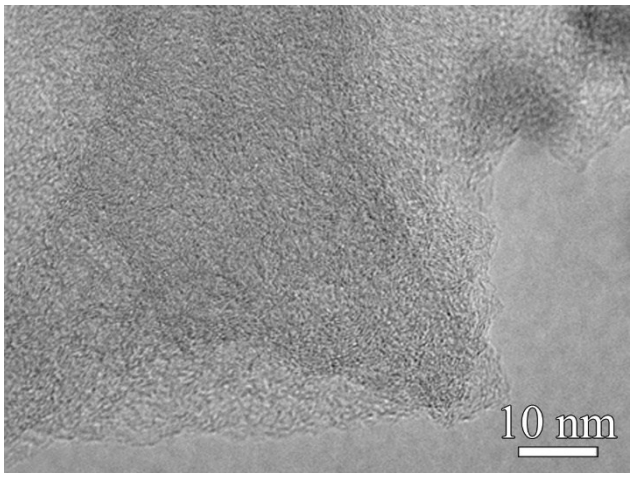

Figure S5. HRTEM image of the well-ordered 3D porous PC.

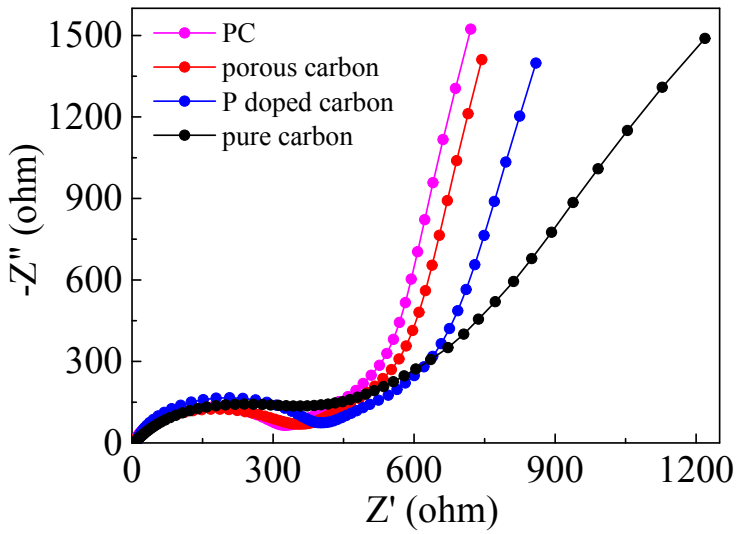

Figure S6. Electrochemical impedance spectra of PC, porous carbon, P doped carbon, and pure carbon as electrodes after fist cycle in the frequency range from 1 MHz to 100 mHz, respectively.

Furthermore, 3D well-ordered porous structure carbon without phosphorus dopants (porous carbon), phosphorus doped carbon (P doped carbon) and pure carbon were prepared. The electrochemical impedance spectra (EIS) of the samples after first cycle are shown in Figure S6. It can be seen that the semicircle diameter in high-medium frequencies for PC is smaller than the other electrodes, indicating the lower charge transfer resistance of PC.

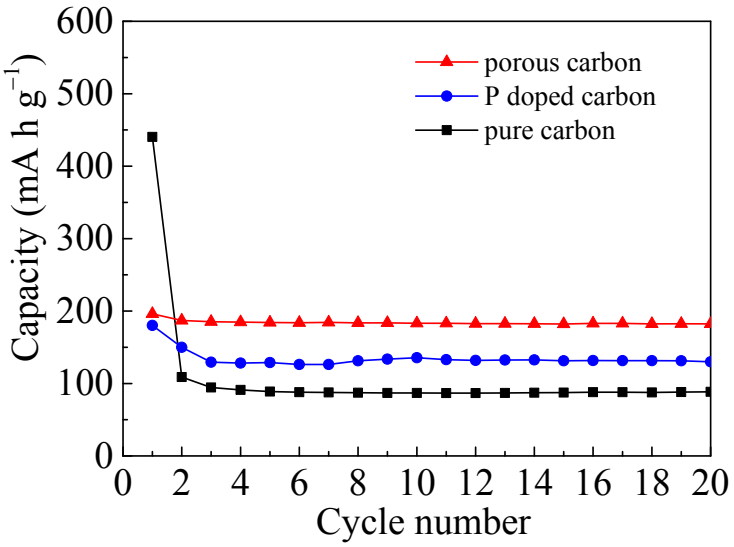

Figure S7. Cycling performance of porous carbon, P doped carbon and pure carbon at a current density of 0.2 A g^{-1}.

The cycling stabilities of porous carbon, P doped carbon, and pure carbon as electrodes were further investigated at a current density of 0.2 A g^{-1}, as shown in Figure S7. The specific capacities of porous carbon, P doped carbon and pure carbon are 182.3, 130.0, and 88.5 mA h g^{-1} after 20 cycles, which are lower than that of PC electrode in Figure 2, indicating both the 3D well-ordered porous structure and the phosphorus doping are helpful to improve the electrochemical performance.

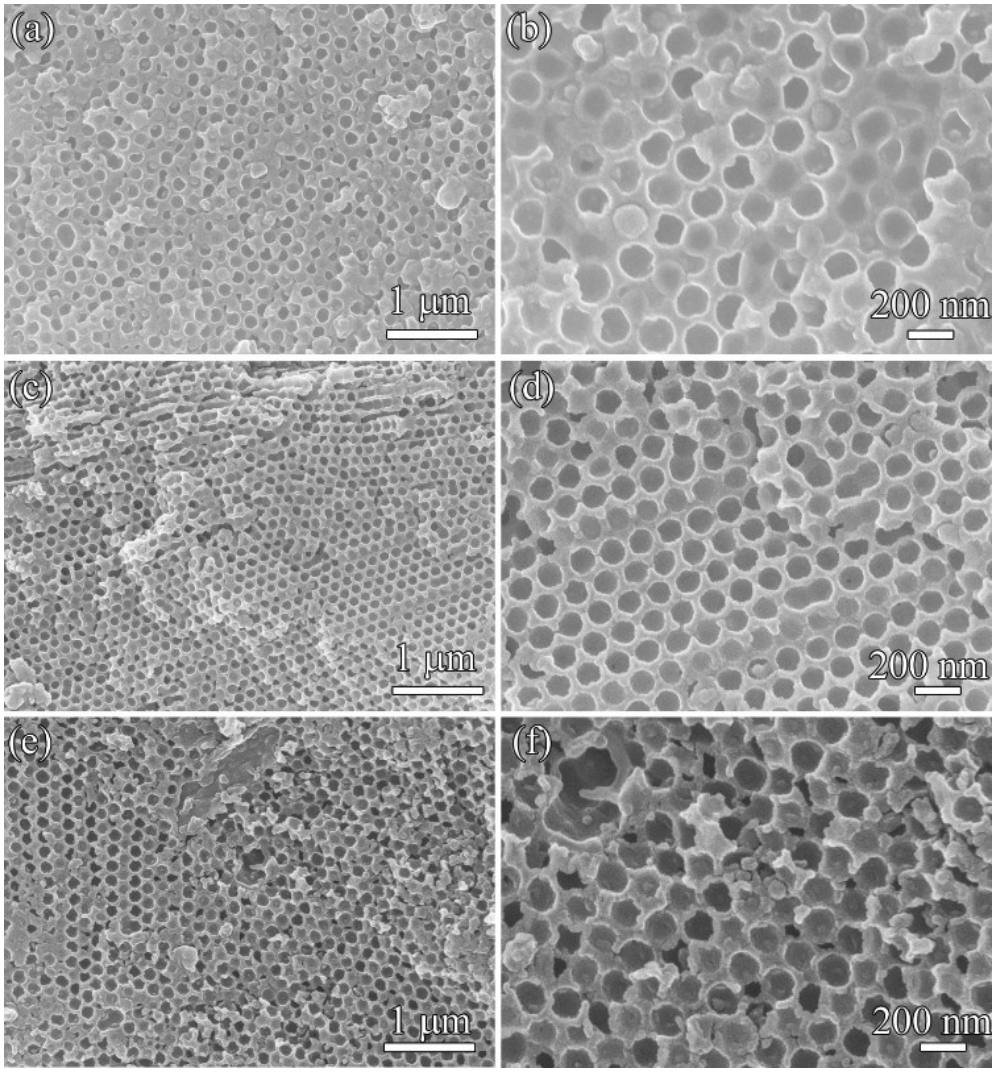

Figure S8. SEM images of (a, b) PC-600, (c, d) PC-700 and (e, f) PC-900.

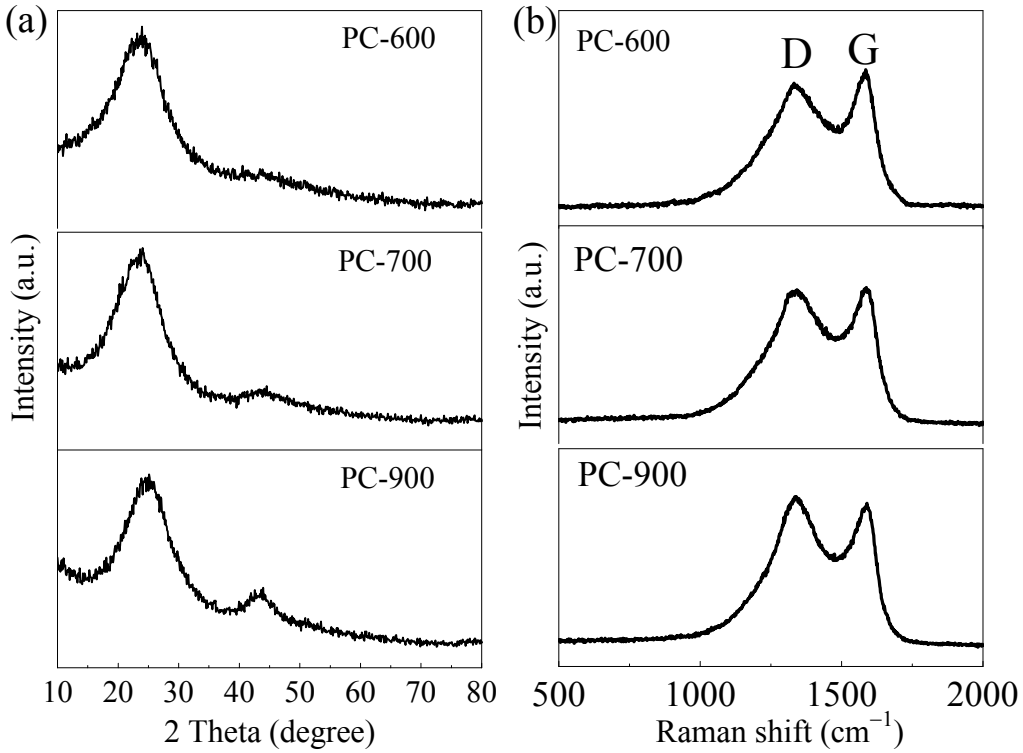

Figure S9. (a) XRD patterns (b) Raman spectra for PC-600, PC-700 and PC-900.

The interlayer distance of PC-600, PC-700 and PC-900 are calculated to be 0.373, 0.369 and 0.357 nm, respectively. It can be seen that the interlayer distance of PCs is larger than that of graphite (0.336 nm), which is essential for the reversible storage of sodium. Meanwhile, the I_D/I_G for PC-600, PC-700 and PC-900 are 1.09, 1.45 and 1.14, respectively, manifesting the disordered structure.

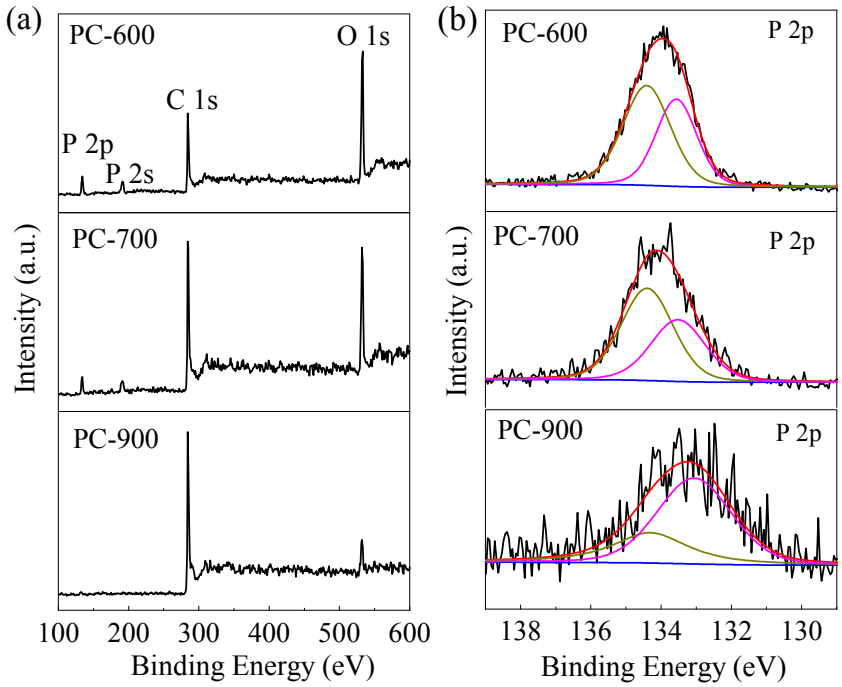

Figure S10. (a) The survey XPS spectra shows that the samples are composed with carbon, oxygen, and phosphorus. (b) High-resolution XPS spectra of the samples also demonstrates the successfully doping of phosphorus into carbon materials.

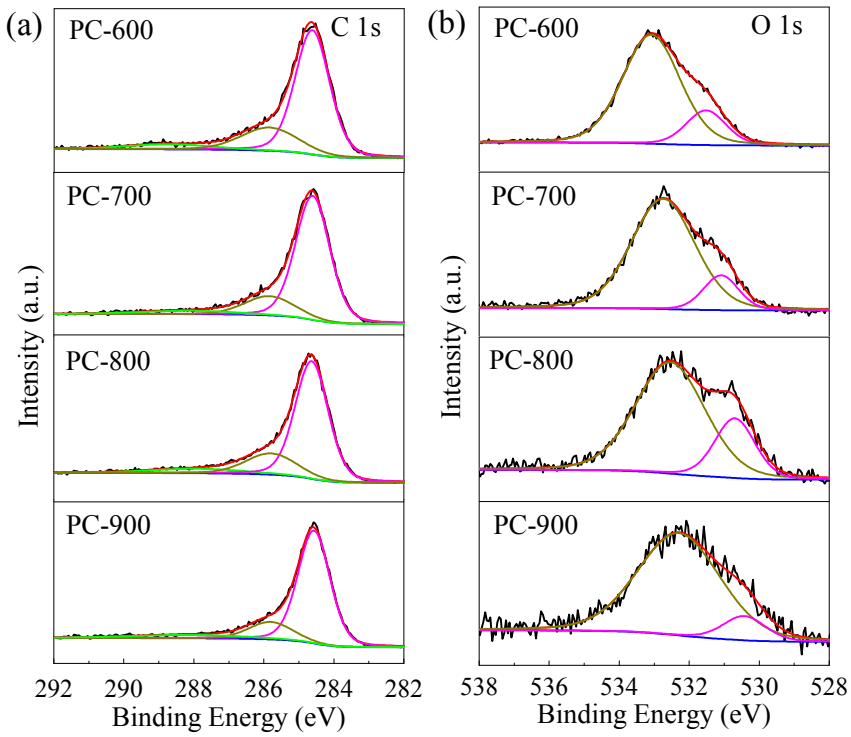

Figure S11. High-resolution XPS spectra of (a) C 1s and (b) O 1s for PC-600, PC-700, PC-800 and PC-900.

The high resolution of C 1s spectra in Figure S11a can be fitted into three peaks at 284.6 eV, 285.8 eV and 288.2 eV, assigning to C-C, C-P and C=O, respectively. The high resolution of O 1s spectra in Figure 118b can be fitted into two peaks at 530.7 eV, and 532.3 eV, assigning to C=O, P=O and O–C–O, C–O–P, respectively. All these results prove the phosphorus can be successfully doped into carbon materials and partially oxidized, in consistent with the high resolution XPS spectra of P 2p.

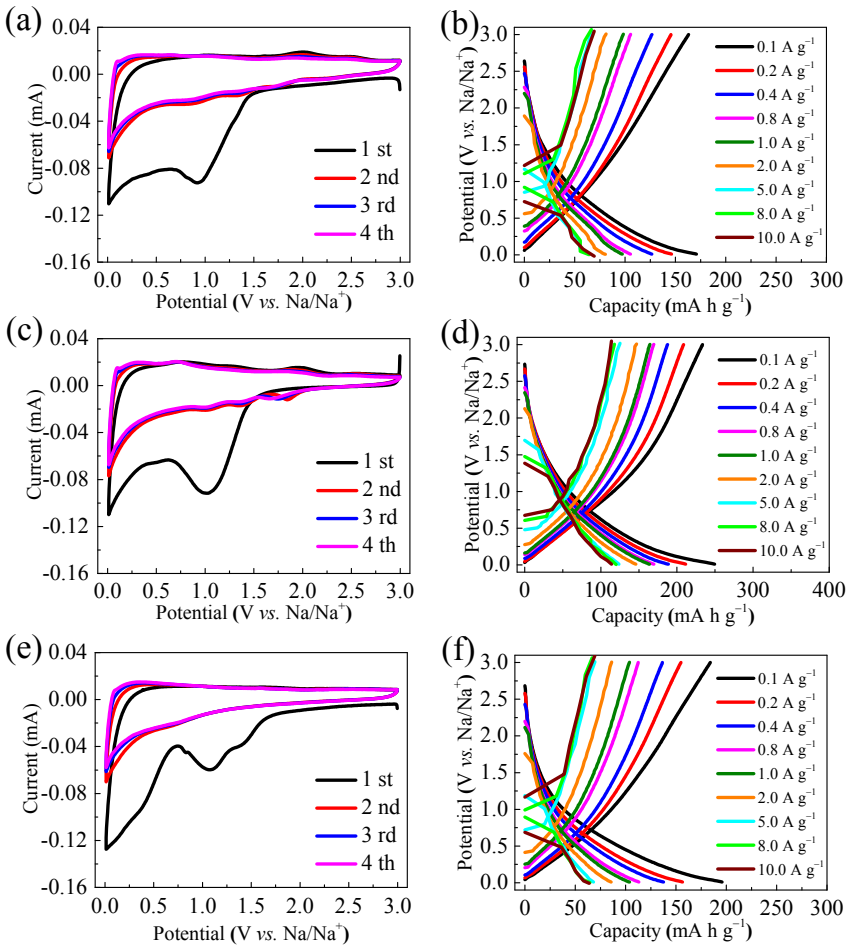

Figure S12. First four cyclic voltammetry (CV) curves of (a) PC-600 (c) PC-700 and (e) PC-900 for the first four cycles in the potential range of 0.0–3.0 V *vs*. Na^+/Na at a scan rate of 0.2 mV s^{-1}; galvanostatic charge and discharge profiles of (b) PC-600 (d) PC-700 and (f) PC-900 at 0.2 A g^{-1}.

As shown in Figure S12a, 9c and 9e, the CV curves of other three samples are similar with well-order 3D porous PC. Two peaks at around 0 V and 1.1 V are corresponding to the insertion/extraction of Na^+ in the hard carbon and the reaction between sodium ions and surface functional groups, respectively. Nevertheless, it can be seen that there are several oxidation/reduction peaks from the second to the forth CV cycles in PC-600 and PC-700, indicative of the pseudocapacitance contribution. Figure S12b, 9d and 9f and Figure S13 show

the discharge and charge profiles of the 5th cycle for the electrodes at each current density, respectively. It can be seen that the polarization in PC-600, PC-900 is more serious, especially at high current density. Higher or lower temperature would reduce the electrochemical performance, and the temperature at 700 ℃, and 800 ℃ are conducive to electrochemical performance.

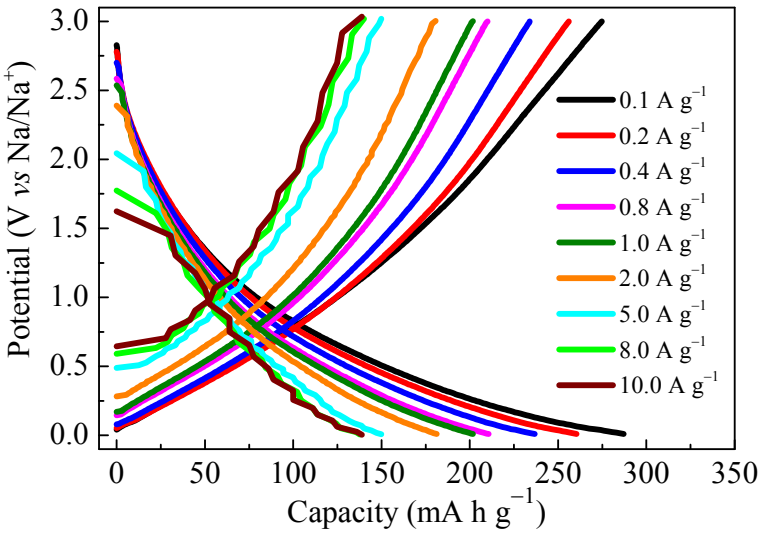

Figure S13. Discharge and charge profiles of the 5th cycle at various current densities for well-ordered 3D porous PC.

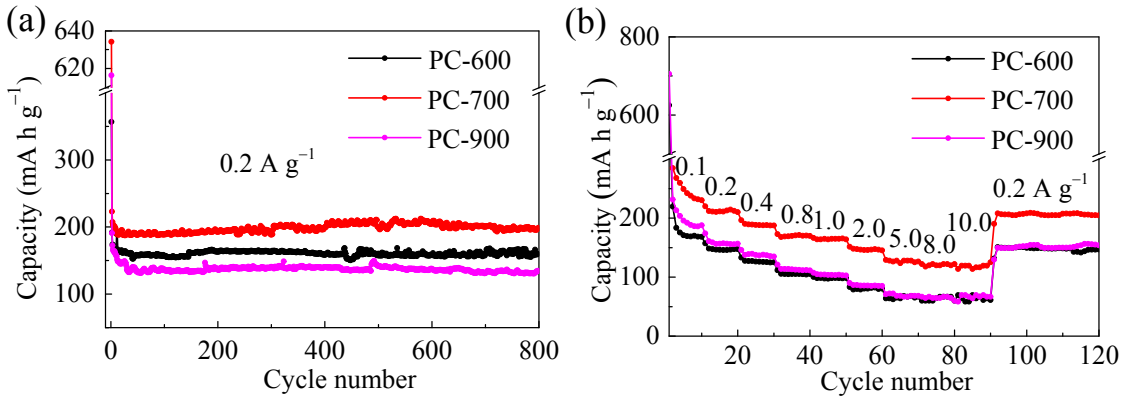

Figure S14. (a) Cycle performance at the current density of 0.2 A g^{-1} (b) Rate performance in the potential range of 0–3.0 V for PC-600, PC-700 and PC-900.

Figure S14a show the cycling performance of the samples at a current density of 0.2 A g^{-1}. The specific capacities are 160, 200 and 150 mA h g^{-1} for PC-600, PC-700 and PC-900, respectively. Where the really interesting difference between the well-ordered 3D porous PC and other three specimens reflects in their rate capability, shown in Figure 2j and Figure S14b. At high charge rates, such as at 10.0 A g^{-1}, the PC-600 and PC-900 samples show effectively negligible capacity. Conversely the PC-800 still has a capacity of 140 mA h g^{-1}. Consequently, these results indicate well-ordered 3D porous PC have excellent electrochemical performance even at high current densities. Obviously, well-ordered 3D porous PC sample performs the best sodium storage capacity.

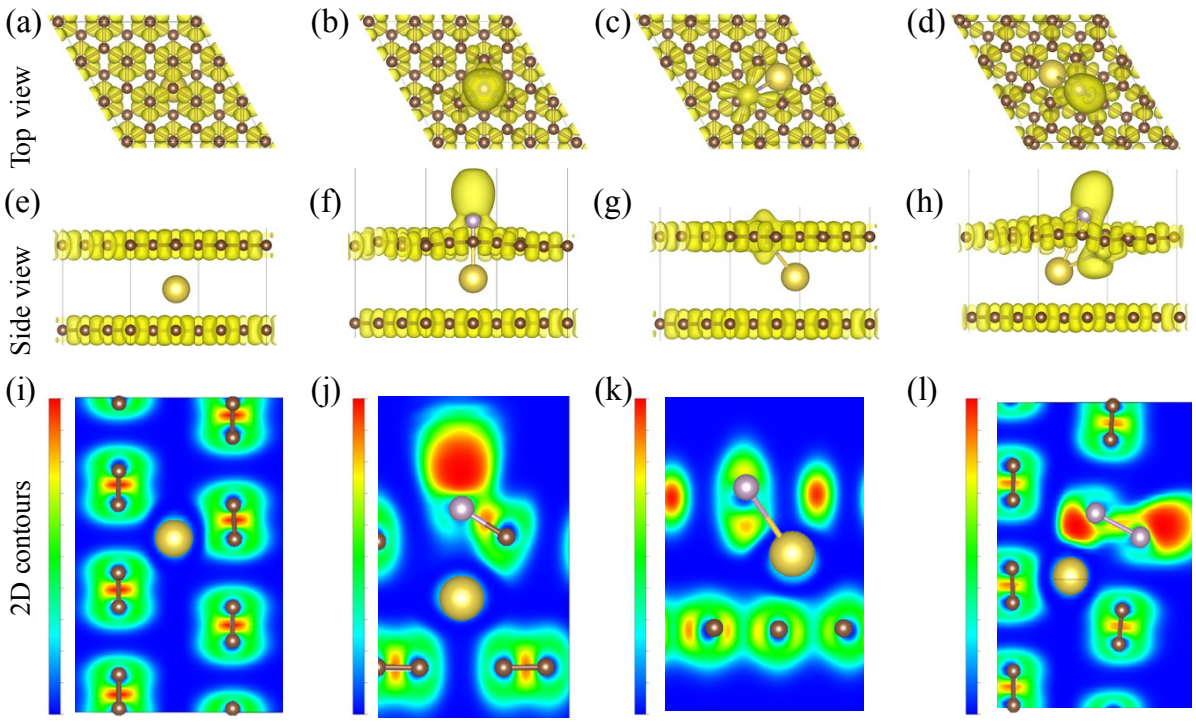

Figure S15. The electron localization function (ELF) of the sodium ion adsorption on (a, c, e) pure graphene, (b, f, j) one carbon atoms replaced by one phosphorus dopant (1P-1C), (c, g, k) two carbon atoms replaced by one phosphorus dopant (1P-2C), (d, h, l) two carbon atoms replaced by two phosphorus dopants (2P-2C). In which, the iso-surface value is 0.50 e $Å^{-3}$; Red, green and blue colors in 2D contours are correspond to ELF values of 1, 0.5 and 0, respectively.

Table S1. the formation energy(E_f) of the phosphorus doped bilayer graphene and the adsorption(E_{ad}) of the bilayer graphene without and with various P dopants.

	pure graphene		
size of supercell	3×3	4×4	5×5
E_f/eV	0	0	0
E_{ad}/eV	1.32	1.10	0.34
	1P-1C		
size of supercell	3×3	4×4	5×5
E_f/eV	-0.51	-0.66	-0.64
E_{ad}/eV	1.87	1.77	1.69
	1C-2P		
size of supercell	3×3	4×4	5×5
E_f/eV	0.79	0.56	0.76
E_{ad}/eV	2.04	1.82	1.87
	2C-2P		
size of supercell	3×3	4×4	5×5
E_f/eV	-2.78	-2.74	-2.64
E_{ad}/eV	1.85	1.74	1.36